Band lineups and deformation potentials in the model-solid theory

Chris G. Van de Walle*
IBM Research Division, Thomas J. Watson Research Center, P. O. Box 218, Yorktown Heights, New York 10598
(Received 13 June 1988; revised manuscript received 3 October 1988)

Semiconductor heterojunctions and superlattices have recently shown tremendous potential for device applications because of their flexibility for tailoring the electronic band structure. A theoretical model is presented to predict the band offsets at both lattice-matched and pseudomorphic strained-layer interfaces. The theory is based on the local-density-functional pseudopotential formalism and the "model-solid approach" of Van de Walle and Martin. This paper is intended as a self-contained description of the model, suitable for practical application. The results can be most simply expressed in terms of an "absolute" energy level for each semiconductor and deformation potentials that describe the effects of strain on the electronic bands. The model predicts reliable values for the experimentally observed lineups in a wide variety of test cases and can be used to explore which combinations of materials and configurations of the strains will lead to the desired electronic properties.

I. INTRODUCTION

In recent years, tremendous developments have occurred in the field of semiconductor heterojunctions and superlattices and their applications in electronic devices. The introduction and improvement of novel growth techniques (in particular, molecular-beam epitaxy) have made it possible to produce extremely high-quality epitaxial interfaces, not only between lattice-matched semiconductors, but even between materials which differ in lattice constant by several percent. Such a lattice mismatch can be accommodated by uniform lattice strain in sufficiently thin layers.[1] The resulting so-called "pseudomorphic" interface is characterized by an in-plane lattice constant which remains the same throughout the structure. These strains can cause profound changes in the electronic properties, and therefore provide extra flexibility in device design. Knowledge of the discontinuities in valence and conduction bands at semiconductor interfaces is essential for the analysis of the properties of any heterojunction, but has remained rather limited due to experimental difficulties, and the absence of reliable theoretical predictions.

Only recently has it become possible to perform first-principles calculations of the band offsets at a semiconductor interface. Such calculations, based on local-density-functional theory and *ab initio* pseudopotentials, have been carried out for a wide variety of lattice-matched interfaces,[2] and also for representative examples of strained-layer interfaces.[3] Unfortunately, the computational complexity of such calculations is very high, which limits their use as a tool in the exploration and design of novel heterostructures. Particularly in the case of strained-layer interfaces, carrying out a self-consistent calculation for every imaginable strain configuration would be unfeasible. This clearly illustrates the need for a reliable model theory that can predict band offsets for a wide variety of interfaces without the need for heavy calculations. Several model theories have been developed in the past, with variable degrees of success.[4] The so-called "model-solid" theory that will be discussed here yields results for lattice-matched interfaces which are at least as good as those achieved by other model theories. Even more importantly, it provides a natural way of dealing with strained-layer interfaces. None of the other model theories includes a prescription for incorporating strain; attempts to add these effects *a posteriori* have not been very successful so far. Particular attention will therefore be paid in this paper to the features of the model-solid theory that allow us to examine strained layers.

A theory that can predict the band lineups at interfaces in the presence of strains should also be able to predict the behavior of valence and conduction bands under strain in a single semiconductor; the shifts of the band edges under strain are described by deformation potentials. It is important to make the distinction between deformation potentials which describe changes in the *relative* energies of different electronic states, and the so-called band-edge deformation potentials, which describe shifts of particular states with respect to a fixed reference energy. It is the latter type of deformation potentials that enters in expressions for electron-phonon scattering.[5] The dilations associated with longitudinal waves in a crystal induce shifts in conduction and valence bands, which affect the carrier mobilities. This effect can be described in terms of scattering by a potential, which is proportional to the volume changes introduced by the acoustic phonon.

Changes in *relative* energies of different states in the same macroscopic region of the crystal (for instance, band-gap changes under pressure) can be measured or calculated with conventional techniques. Changes in the band energies with respect to an *absolute* reference, however, are much harder to derive; the problem is actually similar to that of deriving the band offsets at interfaces. This connection between heterojunction theory and the deformation potential problem was pointed out by Martin,[6] and values for deformation potentials in representa-

tive semicondutors have been obtained using self-consistent interface calculations.[7] Here we will see that the results we obtain from the model theory directly lead to values for the band-edge deformation potentials; we will compare them to the experimental evidence that has recently become available, with promising results.

The model theory, and its connection to the full self-consistent first-principles calculations, has been described in detail elsewhere.[2,8,9] Those references also contain more background on the reasons why the model-solid theory works, and a discussion and comparison with other models. Here I will only briefly summarize the underlying theory, and concentrate on its applications. Section II discusses the structure of the interface, and devotes particular attention to the determination of strains in strained-layer systems. Section III describes how to derive band lineups for arbitrary materials combinations. In Sec. IV we focus attention on the effects of shear strain on the band offsets. Various examples of interfaces that have recently attracted experimental attention are discussed in Sec. V. Section VI concludes the paper.

II. ATOMIC STRUCTURE OF THE INTERFACE—STRAINS

Before we can analyze the electronic structure of an interface, we must define exactly what the positions of the atoms are. First, let me point out that throughout this paper all interfaces are assumed to be ideal, i.e., the bulk atomic structure of each of the semiconductors is maintained up to the interface. This completely defines the structure of any lattice-matched interface. Imperfections (such as impurities, dislocations, . . .) can influence the values of the band lineups in many ways which are generally not yet understood. The first step, however, is to obtain values for the band lineups at ideal interfaces. For strained-layer interfaces, one must include the appropriate strains in each of the materials to construct a pseudomorphic interface. Furthermore, the atomic positions in the neighborhood of the interface are not *a priori* known here, even though only the case of perfect pseudomorphic (commensurate) dislocation-free interfaces is considered. Practical growth of such structure is only possible for layers that do not exceed a certain critical thickness; this thickness depends on the material and on the degree of lattice mismatch. The determination of this critical thickness is an interesting experimental and theoretical problem in itself that is not discussed here.

Since the thickness of the layers in modern multilayer structures can be very small (down to a few monolayers), the problem of determining the structure is one that should be treated on the level of a quantum-mechanical energy minimization of the macroscopic system with respect to the various parameters (strains and atomic displacements). Such a study was performed for the prototypical case of a Si/Ge heterojunction,[3] with results that are expected to be of general validity, and that have been confirmed by experimental observations.[10] The major conclusion is that the structure of the interface can, to a very good approximation, be determined using macroscopic theory. The following description of the procedure is similar to Sec. II of Ref. 3, but is included here for completeness and to establish notation.

The strains in a pseudomorphic (or commensurate) system can be determined by minimizing the macroscopic elastic energy, under the constraint that the lattice constant in the plane, $a_{\parallel}$, is the same throughout the structure (I denote the lattice constant by the symbol a; the subscripts $\parallel$ and $\perp$ are used to indicate quantities parallel or perpendicular to the plane of the interface). We will derive the strain tensors $\vec{\epsilon}$, in each of the materials; we can avoid choosing a particular coordinate system at this point by expressing the tensor components parallel and perpendicular to the plane of the interface. For a system in which h_1 and h_2 are the respective thicknesses of the (unstrained) layers of semiconductors 1 and 2, this yields the following results:

$$a_{\parallel}=\frac{a_1G_1h_1+a_2G_2h_2}{G_1h_1+G_2h_2}\ , \tag{1a}$$

$$\epsilon_{i\parallel}=\frac{a_{\parallel}}{a_i}-1\ , \tag{1b}$$

$$a_{i\perp}=a_i[1-D_i(a_{\parallel}/a_i-1)]\ , \tag{2a}$$

$$\epsilon_{i\perp}=\frac{a_{i\perp}}{a_i}-1\ , \tag{2b}$$

where i denotes the material (1 or 2), a_i denotes the equilibrium lattice constants, and G_i is the shear modulus,

$$G_i=2(c^i_{11}+2c^i_{12})(1-D_i/2)\ . \tag{3}$$

The constant D depends on the elastic constants c_{11}, c_{12}, and c_{44} of the respective materials, and on the interface orientation,

$$D^{001}=2\frac{c_{12}}{c_{11}}\ , \tag{4a}$$

$$D^{110}=\frac{c_{11}+3c_{12}-2c_{44}}{c_{11}+c_{12}+2c_{44}}\ , \tag{4b}$$

$$D^{111}=2\frac{c_{11}+2c_{12}-2c_{44}}{c_{11}+2c_{12}+4c_{44}}\ . \tag{4c}$$

Note that for orientations other than the (001) $a_{\parallel}$ and $a_{\perp}$ do not represent the actual lattice constant in the crystallographic plane of the interface, but merely express how the dimensions of the unit cell change under strain, as given by Eqs. (1b) and (2b).

Equation (1) allows us to observe that when $h_1/h_2\rightarrow\infty$, then $a_{\parallel}\rightarrow a_1$; this corresponds to a substrate of semiconductor 1 with a strained overlayer of semiconductor 2. In general, if a thin overlayer is grown on a substrate, the value of $a_{\parallel}$ is determined by the substrate and may be varied by using different substrates. However, for free-standing superlattices $a_{\parallel}$ must be determined using Eq. (1). Once $a_{\parallel}$ is known, $a_{i\perp}$ can be obtained using Eq. (2).

Those formulas determine the strains in the layers, and all atomic positions, except the interatomic distance at the interface itself. The first-principles total-energy calculations showed that the interplanar separation between the outermost layers of semiconductors 1 and 2 at the in-

terface is close to the average of the layer spacings in the two (appropriately strained) bulk materials.

For the (111) and (110) interfaces, strains reduce the crystal symmetry in such a way that the separation of the two atoms in the bulk unit cell of the diamond or zinc blende structure is not uniquely determined from the macroscopic strain. When the materials are distorted along these directions, internal displacements of the atoms occur.[11] These displacements are described by a parameter ζ, and can have an important effect on the magnitude of certain deformation potentials that describe splittings of degenerate bands under shear strain. The exact knowledge of the atomic positions is not required for application of the theory that I will present; only macroscopic quantities, such as strains, will enter. It is important, however, to realize that effects such as internal displacements do occur, and that they are properly included in the calculated values that will be presented.

Table I lists values of lattice constants and elastic constants for a wide variety of semiconductors. Some of the values for lattice constants are slightly different from the exact experimental values. That is because, in an attempt to establish classes of closely lattice-matched materials, I decided to neglect any mismatch that is less than $\sim 0.5\%$. Such a small mismatch would only lead to strain effects in the lineups which are significantly smaller than the accuracy of the present calculations (and of most experimental measurements). Many of the references for elastic constants were obtained through the Landolt-Börnstein tables.[25] Where available, low-temperature values were used. For convenience, I also give the values of the constants D and G for different interface orientations, as defined in Eqs. (3) and (4),

Examples. Using these values, and appropriate information on boundary conditions or layer thicknesses, a determination of the strains with Eqs. (1) and (2) is straightforward. Let us illustrate the procedure for a ZnS/ZnSe (001) interface: first, consider the case of a thin ZnS overlayer on a ZnSe substrate. This fixes $a_{\parallel}=5.65$ Å; no strains are present in ZnSe. Further,

$$\epsilon_{\mathrm{ZnS}\parallel}=\frac{5.65}{5.40}-1=0.046 ,$$

$$\epsilon_{\mathrm{ZnS}\perp}=-1.248\times 0.046=-0.058 ,$$

and

$$a_{\mathrm{ZnS}\perp}=5.09 \text{ Å} .$$

If we choose a Cartesian coordinate system with x and y axes in the plane of the interface, and z axis perpendicular to the interface [hence the notation (001)], the components of the strain tensor for ZnS are $\epsilon_{xx}=\epsilon_{yy}=0.046$, $\epsilon_{zz}=-0.058$. All off-diagonal components are zero. This results in a volume change $\Delta\Omega/\Omega=\mathrm{Tr}(\overleftrightarrow{\epsilon})=0.035$. This volume change determines the hydrostatic contribution of the strain, and will enter into the overall band lineups. The nonhydrostatic strain components (shear strains), which determine the uniaxial (or biaxial) strains, will cause splittings of degenerate bands.

As a second example, we consider a superlattice with equally thick layers ($h_{\mathrm{ZnSe}}=h_{\mathrm{ZnS}}$). Equation (1) yields

$$a_{\parallel}=\frac{(5.65)(1.447)+(5.40)(1.803)}{1.447+1.803}=5.51 \text{ Å} .$$

TABLE I. Lattice constant a (in Å) and elastic constants c_{11}, c_{12}, and c_{44} for various diamond and zinc-blende structure semiconductors. Also given are values of the parameters G and D for different interface orientations, as defined in Eqs. (1) and (2). The elastic constants and G are given in Mbar; D is dimensionless.

	a	c_{11}	c_{12}	c_{44}	D^{001}	G^{001}	D^{110}	G^{110}	D^{111}	G^{111}
Si[a]	5.43	1.675	0.650	0.801	0.776	3.641	0.515	4.417	0.444	4.628
Ge[a]	5.65	1.315	0.494	0.684	0.751	2.876	0.450	3.570	0.371	3.751
GaAs[b]	5.65	1.223	0.571	0.600	0.934	2.522	0.580	3.359	0.489	3.574
AlAs[c]	5.65	1.250	0.534	0.542	0.854	2.656	0.616	3.207	0.550	3.361
InAs[d]	6.08	0.833	0.453	0.396	1.088	1.587	0.674	2.306	0.570	2.487
GaP[e]	5.43	1.439	0.652	0.714	0.906	3.000	0.559	3.953	0.470	4.198
AlP[c]	5.43	1.320	0.630	0.615	0.955	2.697	0.623	3.554	0.536	3.778
InP[f]	5.87	1.022	0.576	0.460	1.127	1.897	0.727	2.768	0.625	2.990
GaSb[g]	6.08	0.908	0.413	0.445	0.910	1.891	0.569	2.482	0.480	2.635
AlSb[h]	6.08	0.877	0.434	0.408	0.990	1.763	0.641	2.372	0.550	2.530
InSb[i]	6.48	0.659	0.356	0.300	1.080	1.261	0.698	1.785	0.600	1.920
ZnSe[j]	5.65	0.826	0.498	0.400	1.206	1.447	0.716	2.340	0.597	2.556
ZnS[k]	5.40	1.067	0.666	0.456	1.248	1.803	0.814	2.845	0.704	3.109
ZnTe[j]	6.08	0.713	0.407	0.312	1.142	1.311	0.751	1.907	0.651	2.060
CdTe[l]	6.48	0.562	0.394	0.206	1.402	0.807	0.974	1.386	0.863	1.535
HgTe[m]	6.48	0.597	0.415	0.226	1.390	0.870	0.949	1.499	0.837	1.660

[a]Reference 12.
[b]Reference 13.
[c]Reference 14.
[d]Reference 15.
[e]Reference 16.
[f]Reference 17.
[g]Reference 18.
[h]Reference 19.
[i]Reference 20.
[j]Reference 21.
[k]Reference 22.
[l]Reference 23.
[m]Reference 24.

Strain components can easily be obtained from Eqs. (1b) and (2).

I end this section with a word of caution. The model-solid theory, as I will describe it, performs very well in its predictions for band offsets at ideal interfaces. While many of the present technologically important heterojunctions fall into that category, it should be kept in mind that certain classes of interfaces may significantly deviate from ideality. One example is that of interfaces between a group-IV element and a III-V or II-VI compound, or between compounds which do not have any elements (cations nor anions) in common. The (110) orientation poses no problem for these systems, since it is nonpolar and avoids charge accumulation at the interface; however, the (001) or (111) orientations are polar in nature and require atomic mixing of the semiconductors at the interface.[26] It has been shown that different types of mixing can set up different dipoles, which significantly alter the band lineups.[27] Effects of this nature are clearly beyond the scope of the model-solid theory, and indeed of *any* theory which relies on the lineup of reference levels which are *intrinsic* to the bulk materials. One can, in principle, describe the effect in terms of certain dipoles, which would be added on to the model-solid lineup. Such dipoles, induced by atomic rearrangements, could conceivably also become significant in cases where a common anion is present, such as for (001) or (111) oriented strained-layer interfaces, or at an interface such as ZnSe/Ge, where the difference in Zn-Ge versus Se-Ge bondlengths could drive atomic displacements. While no specific cases have been reported so far where the model-solid approach would break down, one should always bear in mind what its underlying assumptions and consequently its limitations are.

III. MODEL-SOLID THEORY

The model-solid theory has two main aspects: first, the generation of an accurate band structure, and second, the alignment of this band structure on an "absolute" energy scale. The first part is accomplished by performing density-functional calculations[28] on individual bulk semiconductors,[29] described by *ab initio* pseudopotentials.[30] The accuracy and margin of error of band structures produced by these calculations is well established by now, and changes in the bands induced by hydrostatic or shear strains are reliably predicted. The calculated band structures include scalar relativistic effects (included through the use of the pseudopotentials of Ref. 30), but no spin-orbit splitting effects; these will be added *a posteriori*. A discussion of intrinsic deficiencies of density-functional theory and their effect on band lineups was presented in Refs. 2 and 3. The best-known deficiency is the failure of density-functional theory to produce the correct band gap.[31] Our procedure has been to use the calculated valence-band position, and then add the experimental band gap to obtain conduction-band positions. Even the valence-band positions themselves may be subject to certain errors within local-density-functional theory. However, these errors are expected to be smaller than those for conduction bands, and similar in magnitude for most of the semiconductors that are studied here.[32] They therefore tend to cancel when we look at *differences*, as in the band-lineup problem. The largest errors are expected to occur in the case of lineups between semiconductors with very different ionicities; in particular, heterojunctions between group-IV or III-V semiconductors on the one side, and II-VI compounds on the other side should be treated with caution.

The second part of the problem is that of establishing an absolute energy scale. Such an absolute reference can only be present when the energies in the bulk semiconductor can be referred to the "vacuum level." Since typical bulk calculations are carried out for an infinite crystal, no such reference is available; the calculated energy bands are referred to an average electrostatic potential within the solid, which is only defined to within an arbitrary constant.[33] The principal feature of the model-solid theory consists of a particular way of relating this average electrostatic potential to the vacuum level. This puts all calculated energies on an absolute energy scale, and allows us to derive band lineups by simply subtracting values for individual semiconductors. The common reference is accomplished by modeling the solid as a superposition of neutral atoms. In each atom, the electrostatic potential is rigorously defined with respect to the vacuum level. The average electrostatic potential in this "model solid" is therefore, by superposition, also well specified on the absolute energy scale.[34] I should emphasize that this choice of an absolute energy scale is by no means unique. It is, however, well defined by the prescription of superposition of neutral atomic[35] charge densities, calculated within the local-density approximation (LDA) for the pseudopotentials that are used in the band-structure calculations.[30]

Taken separately, the results for band position with respect to the average potential and for the average potential itself contain no information, since they depend on the choice of pseudopotential and of angular momentum used for the local part of the the potential. Only the combination of both, which gives the band positions on an absolute energy scale, is meaningful and independent of choices in the pseudopotential. Table II contains an overview of all results for elemental, III-V and II-VI semiconductors. Listed in the table are values for $E_{v,\mathrm{av}}$, which is the average over the three uppermost valence bands at Γ (known as the light and heavy hole bands, and the spin-orbit split-off band). The reason I introduce this average is that splittings of the valence bands will occur due to shear strains and/or spin-orbit splittings. These splittings can be easily expressed in formulas that refer the individual bands to the average. In the first step, it is therefore convenient to determine the position of $E_{v,\mathrm{av}}$. I stress that these "absolute" values for $E_{v,\mathrm{av}}$ do not carry any physical meaning when taken by themselves, and should certainly not be related to the ionization potential. They are only meaningful relative to similar quantities in other semiconductors.

Besides the position of the (average) valence band on an absolute energy scale, $E_{v,\mathrm{av}}$, the model-solid approach can also give us information about the variation of this energy when strain is present in the system. Shear components of the strain can have a profound effect on de-

TABLE II. Spin-orbit splittings Δ_0, and energy gaps E_g of various semiconductors (Ref. 25). Values of $E_{v,\mathrm{av}}$ (average of three uppermost valence bands at Γ), $a_v = d(E_{v,\mathrm{av}})/d(\ln\Omega)$, $a_c = d(E_c)/d(\ln\Omega)$, and $a = d(E_c - E_{v,\mathrm{av}})/(d\ln\Omega)$ are calculated within the model-solid approach. For indirect-gap semiconductors, values of E_g, E_c, a_c, and a are given for both direct and indirect gaps.

	Δ_0	$E_{v,\mathrm{av}}$	a_v	E_g^{dir}	E_c^{dir}	a_c^{dir}	a^{dir}	E_g^{ind}	E_c^{ind}	a_c^{ind}	a^{ind}
Si	0.04	−7.03	2.46	3.37	−3.65	1.98	−0.48	1.17	−5.85	4.18	1.72
Ge	0.30	−6.35	1.24	0.89	−5.36	−8.24	−9.48	0.74	−5.51	−1.54	−2.78
GaAs	0.34	−6.92	1.16	1.52	−5.29	−7.17	−8.33				
AlAs	0.28	−7.49	2.47	3.13	−4.27	−5.64	−8.11	2.23	−5.17	4.09	1.62
InAs	0.38	−6.67	1.00	0.41	−6.13	−5.08	−6.08				
GaP	0.08	−7.40	1.70	2.90	−4.47	−7.14	−8.83	2.35	−5.02	3.26	1.56
AlP		−8.09	3.15	3.63	−4.46	−5.54	−8.70	2.51	−5.58	5.12	1.97
InP	0.11	−7.04	1.27	1.42	−5.58	−5.04	−6.31				
GaSb	0.82	−6.25	0.79	0.75	−5.23	−6.85	−7.64				
AlSb	0.65	−6.66	1.38	2.32	−4.12	−6.97	−8.36	1.70	−4.74	3.05	1.67
InSb	0.81	−6.09	0.36	0.24	−5.58	−6.17	−6.53				
ZnSe	0.43	−8.37	1.65	2.83	−5.40	−4.17	−5.82				
ZnS	0.07	−9.15	2.31	3.84	−5.29	−4.09	−6.40				
ZnTe	0.91	−7.17	0.79	2.39	−4.48	−5.83	−6.62				
CdTe	0.93	−7.07	0.55	1.59	−5.17	−3.96	−4.52				
HgTe	1.05	−6.88	−0.13	−0.30	−6.83	−4.60	−4.48				

generate bands; they lead to splittings of the valence bands (and of indirect conduction bands) which are well described with deformation potential theory, as I will discuss later. These splittings are averaged out, however, when considering the average $E_{v,\mathrm{av}}$, which is subject only to shifts due to the hydrostatic component of the strain (corresponding to a volume change). Once again, two contributions occur in the calculation. On the one hand, there is the effect on the band structure when the solid is compressed; the bands shift with respect to the average potential in the solid. On the other hand, the average electrostatic potential itself is shifted due to the (hydrostatic component of the) strain, because it is inversely proportional to the volume.[34] The total effect leads to a hydrostatic deformation potential for the valence band:

$$a_v = \frac{dE_{v,\mathrm{av}}}{d\ln\Omega} , \tag{5}$$

which expresses the shift in $E_{v,\mathrm{av}}$ per unit fractional volume change (note that $d\ln\Omega = d\Omega/\Omega$). A similar definition applies to the conduction-band deformation potential a_c. The band-gap deformation potential is, of course, equal to $a = a_c - a_v$. Values for a_v, a_c, and a are listed in Table II. I will discuss these and their connection to experiment in more detail in Sec. V.

When dealing with bulk semiconductors, one usually considers only the *relative* shift of the conduction band with respect to the valence band (expressed by the deformation potential a); for the heterojunction problem, however, values for individual band edges are essential, since they influence the discontinuities at the interface. These effects are expressed as

$$\Delta E_{v,\mathrm{av}} = a_v \frac{\Delta\Omega}{\Omega} , \tag{6}$$

where a_v is the hydrostatic deformation potential for the valence band, and $\Delta\Omega/\Omega = \mathrm{Tr}(\overleftrightarrow{\epsilon}) = (\epsilon_{xx} + \epsilon_{yy} + \epsilon_{zz})$ is the fractional volume change. Similarly,

$$\Delta E_c = a_c \frac{\Delta\Omega}{\Omega} . \tag{7}$$

Even when no shear strains are present the valence band is usually split due to spin-orbit effects. The experimental spin-orbit splitting is listed in Table II, and allows us to derive the position of the topmost valence band:

$$E_v = E_{v,\mathrm{av}} + \frac{\Delta_0}{3} . \tag{8}$$

Table II also contains values for conduction-band positions, including indirect conduction-band minima when these determine the lowest gap. They are derived based on valence-band positions and experimental low-temperature gaps (also listed in Table II), with the formula

$$E_c = E_v + E_g , \tag{9}$$

where E_v itself is obtained from Eq. (8).

By comparison with fully self-consistent interface calculations,[2] the error bar on band offsets determined from the model-solid theory is ~ 0.2 eV. The error bar on the values of band-edge deformation potentials is estimated to be ± 1 eV. The list of semiconductors in Table II is divided into several blocks, each of which contains materials with similar characteristics (namely group IV elemental, III-V compound, and II-VI compound semiconductors). The model-solid approach is expected to give the most reliable results for lineups between materials belonging to the same block. When two semiconductors belong to different blocks in Table II, the resulting lineups should be regarded with more caution. I also point out that within the model-solid theory no distinction exists

between different interface orientations. The band lineups at lattice-matched interfaces are therefore independent of interface orientation, which has been confirmed for a large class of interfaces by full self-consistent calculations.[2,36] For strained-layer interfaces, the strains may of course depend on the particular orientation, and thus affect the lineups.

Examples. To conclude this section, let us illustrate how to derive band offsets for a heterojunction A/B starting from the values in Table II. For lattice-matched interfaces, the discontinuity in the average valence bands is simply

$$\Delta E_{v,\mathrm{av}} = E^{B}_{v,\mathrm{av}} - E^{A}_{v,\mathrm{av}} \ . \tag{10}$$

The sign convention is such that $\Delta E_{v,\mathrm{av}}$ is positive when the valence band in B is higher in energy than the valence band in A. To obtain the position of the individual bands with respect to the average, the spin-orbit splitting Δ_0 has to be introduced, as in Eq. (8). As an example, we find for AlSb/GaSb:

$$\Delta E_{v,\mathrm{av}} = (-6.25) - (-6.66) = 0.41 \text{ eV} \ .$$

and

$$\Delta E_v = 0.41 + (0.82/3) - (0.65/3) = 0.47 \text{ eV} \ .$$

Similarly, for the conduction-band discontinuity (which occurs between the direct conduction-band minimum in GaSb and the indirect minimum in AlSb,

$$\Delta E_c = (-5.23) - (-4.74) = -0.49 \text{ eV} \ .$$

The minus sign indicates that the conduction band in GaSb is below the conduction band in AlSb; the lineup is "type I," meaning that the band gap of one material (GaSb) falls completely inside the band gap of the other (AlSb). These lineups are illustrated in Fig. 1.

For strained-layer interfaces, one first has to determine the strain components in each of the materials, as described in detail in Sec. II. Continuing our example of a thin layer of pure ZnS deposited on a (001) ZnSe substrate, we have the strains: $\epsilon_{xx} = \epsilon_{yy} = 0.046$, $\epsilon_{zz} = -0.058$. These result in a volume change $\Delta\Omega/\Omega = 0.035$. The positions of $E_{v,\mathrm{av}}$ and E_c are affected by the volume change in the layers. The relation

$$E_{v,\mathrm{av}} = E^{0}_{v,\mathrm{av}} + a_v \frac{\Delta\Omega}{\Omega} \tag{11}$$

[based on Eq. (6)] expresses $E_{v,\mathrm{av}}$ in terms of its value in the unstrained material (i.e., the equilibrium-volume value from Table II), the hydrostatic deformation potential for the valence band a_v, and the fractional volume change $\Delta\Omega/\Omega = \mathrm{Tr}(\vec{\epsilon}) = (\epsilon_{xx} + \epsilon_{yy} + \epsilon_{zz})$. $\Delta E_{v,\mathrm{av}}$ then follows immediately. Conduction bands can be positioned in a similar manner, using the E_c values listed in Table II, and including the appropriate shifts due to strain.

From Table II and Eq. (6):

$$E^{\mathrm{ZnSe}}_{v,\mathrm{av}} = -8.37 \text{ eV} \ ,$$

and

$$E^{\mathrm{ZnS}}_{v,\mathrm{av}} = -9.15 + 2.31 \times 0.035 = -9.07 \text{ eV} \ .$$

This leads to $\Delta E_{v,\mathrm{av}} = 0.70$ eV (higher in ZnSe). For the conduction bands, we find

$$E^{\mathrm{ZnSe}}_{c} = -5.40 \text{ eV} \ ,$$

and

$$E^{\mathrm{ZnS}}_{c} = E^{\mathrm{ZnS},0}_{c} + a_c \frac{\Delta\Omega}{\Omega}$$

$$= -5.29 + (-4.09)0.035 = -5.43 \text{ eV} \ .$$

This results in $\Delta E_c = 0.03$ eV. The lineups are shown in Fig. 2.

So far, we have only derived $\Delta E_{v,\mathrm{av}}$ for this system. The shear strains in ZnS cause significant splittings of the valence bands. To determine the position of the individual valence bands we must use formulas that properly combine strain and spin-orbit splittings. This will be the subject of Sec. IV.

IV. STRAIN SPLITTINGS AND DEFORMATION POTENTIALS

In Sec. III I described how to obtain band lineups from the model-solid theory, using the values listed in Table II. For strained-layer interfaces, we saw how to include the effects of hydrostatic strain in the overall lineups (for $\Delta E_{v,\mathrm{av}}$); important effects on the band structure also

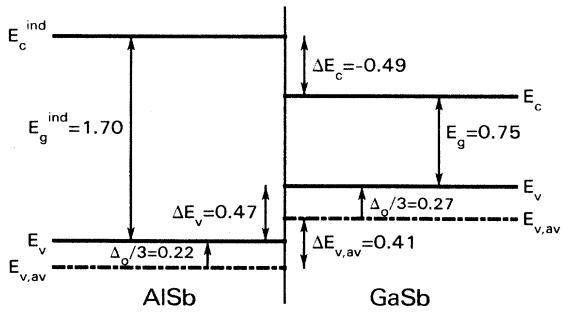

FIG. 1. Band lineups at an AlSb/GaSb interface. The discontinuity in the average valence bands, $\Delta E_{v,\mathrm{av}}$, is obtained from the model-solid theory. Spin-orbit splittings and energy gaps are taken from experiment. All energies are in eV.

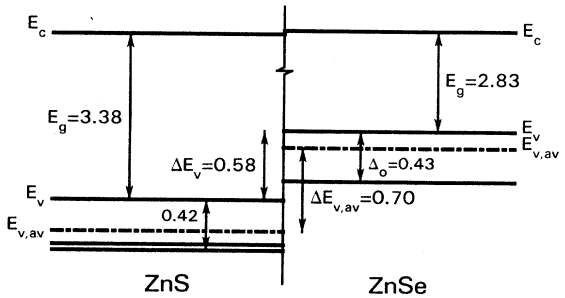

FIG. 2. Band lineups at a ZnS/ZnSe interface. The discontinuity in the average valence bands, $\Delta E_{v,\mathrm{av}}$, is obtained from the model-solid theory. Strain shifts and splittings are described in the text. Spin-orbit splittings and equilibrium energy gaps are taken from experiment. All energies are in eV.

occur, however, due to shear strains which break the symmetry and split otherwise degenerate bands. These effects are well documented in the literature,[37] and their description is independent of the model-solid theory that is used here to line up the overall band structures. Nevertheless, I think it is worthwhile to present the theoretical description here, in the same notation as introduced in previous sections, in order to obtain a comprehensive overview of band-offset calculations for strained-layer interfaces.

A. Valence bands

All the semiconductors discussed here (listed in Table II) have the zinc blende (or diamond) structure, with a band structure that includes three degenerate valence bands at Γ. These bands are strictly degenerate only in the absence of strain and spin-orbit splitting. They are labeled here by $E_{v,1}, E_{v,2}$ (the light and heavy hole bands, respectively), and $E_{v,3}$ (the split-off band). The average of these bands is referred to as $E_{v,\mathrm{av}}$. When no strain is present, spin-orbit effects raise $E_{v,1}$ and $E_{v,2}$ with respect to $E_{v,3}$; the shift of the uppermost bands with respect to $E_{v,\mathrm{av}}$ was described in Eq. (8). Shear components of the strain lead to additional splittings, which interact with the spin-orbit splittings to produce the final valence-band positions. The strain splittings themselves are proportional to the magnitude of the strain, and are well described in terms of deformation potentials.[37] For strain along [001], the following shifts are calculated with respect to the average $E_{v,\mathrm{av}}$:

$$\Delta E_{v,2} = \tfrac{1}{3}\Delta_0 - \tfrac{1}{2}\delta E_{001} , \tag{12a}$$

$$\Delta E_{v,1} = -\tfrac{1}{6}\Delta_0 + \tfrac{1}{4}\delta E_{001} + \tfrac{1}{2}[\Delta_0^2 + \Delta_0 \delta E_{001} + \tfrac{9}{4}(\delta E_{001})^2]^{1/2} , \tag{12b}$$

$$\Delta E_{v,3} = -\tfrac{1}{6}\Delta_0 + \tfrac{1}{4}\delta E_{001} - \tfrac{1}{2}[\Delta_0^2 + \Delta_0 \delta E_{001} + \tfrac{9}{4}(\delta E_{001})^2]^{1/2} . \tag{12c}$$

In these equations δE_{001} is given by

$$\delta E_{001} = 2b(\epsilon_{zz} - \epsilon_{xx}) , \tag{13}$$

where b is the shear deformation potential for a strain of tetragonal symmetry; b is negative for all the semiconductors discussed here. Experimental values for this quantity are available for some but not all semiconductors. The deformation potential b can also be calculated by analyzing changes in the band structure when strain is applied;[3] such theoretical values for b have proven to be reliable. Table III lists experimental and theoretical numbers for many semiconductors.

TABLE III. Theoretical and experimental (Ref. 25, except where indicated) values for deformation potentials b and d for various semiconductors. All values are in eV.

	b (theor)	b (expt)	d (theor)	d (expt)
Si	−2.35	−2.1	−5.32	−4.8
Ge	−2.55	−2.9	−5.50	−5.3
GaAs	−1.90	−1.7	−4.23	−4.5
AlAs				
InAs	−1.55	−1.8	−3.10	−3.6
GaP		−1.5		−4.6
AlP				
InP		−1.6		−4.2
GaSb		−2.0		−4.8
AlSb		−1.4		−4.3
InSb		−2.1		−5.0
ZnSe	−1.20	−1.2[a]		
ZnS	−1.25	−0.8[a]		
ZnTe	−1.26			
CdTe	−1.10	−1.2		−2.8
HgTe	−1.15			

[a]Reference 38.

The total splitting of the bands in the absence of spin-orbit splitting is equal to $\frac{3}{2}|\delta E_{001}|$. Note that Eqs. (12) and (13) were derived in the linear regime, as were all the expressions for strain-induced shifts or splittings in this paper; they might therefore become invalid for large strains. However, the linear approximation is expected to be adequate for any strain that can be achieved in practical pseudomorphic layer growth. The band v_2 is a pure $|\frac{3}{2},\frac{3}{2}\rangle$ state, while v_1 and v_3 are mixtures of $|\frac{3}{2},\frac{1}{2}\rangle$ and $|\frac{1}{2},\frac{1}{2}\rangle$.

The case of uniaxial strain along [111] is very similar; Eqs. (12) remain valid, with δE_{001} replaced by δE_{111}, where

$$\delta E_{111} = 2\sqrt{3} d \epsilon_{xy} \tag{14}$$

with $\epsilon_{xy} = \frac{1}{3}(\epsilon_\perp - \epsilon_\parallel)$. Values for the deformation potential d are listed in Table III. It should be noted that the calculated values of this deformation potential are quite sensitive to the internal displacement parameter which describes displacements of the atoms in the unit cell under (111) strain (see Sec. II). I have used values for this parameter which were calculated with the same methods and potentials as in the present work.[29] The agreement between theory and experiment for d supports the validity of this approach.

The case of unaxial strain along [110] is somewhat more complicated. No analytical expressions can be written down for the energy levels, and the strain splitting is a consequence of a mixture of the deformation potentials b and d. The valence-band positions correspond to the eigenvalues of the matrix:[37]

$$\begin{pmatrix} \frac{\Delta_0}{3} - \frac{1}{8}(\delta E_{001} + 3\delta E_{111}) & -\frac{\sqrt{3}}{8}(\delta E_{001} - \delta E_{111}) & \frac{\sqrt{6}}{8}(\delta E_{001} - \delta E_{111}) \\ -\frac{\sqrt{3}}{8}(\delta E_{001} - \delta E_{111}) & \frac{\Delta_0}{3} + \frac{1}{8}(\delta E_{001} + 3\delta E_{111}) & \frac{\sqrt{2}}{8}(\delta E_{001} + 3\delta E_{111}) \\ \frac{\sqrt{6}}{8}(\delta E_{001} - \delta E_{111}) & \frac{\sqrt{2}}{8}(\delta E_{001} + 3\delta E_{111}) & -\frac{2}{3}\Delta_0 \end{pmatrix} ,$$

where now

$$\delta E_{001}=4b(\epsilon_{xx}-\epsilon_{zz}) \tag{15a}$$

and

$$\delta E_{111}=(4/\sqrt{3})d\epsilon_{xy} . \tag{15b}$$

Example. At this point we can go back to our example of (001) ZnS/ZnSe, and include the strain splitting of the valence band in ZnS. Recalling that $\epsilon_{xx}=\epsilon_{yy}=0.046$ and $\epsilon_{zz}=-0.058$, and using $b=-1.25$ from Table III, we obtain with Eq. (13): $\delta E_{001}=0.26$ eV. Equations (12) then give

$$\Delta E_{v,2}=-0.11 ,$$

$$\Delta E_{v,1}=+0.26 ,$$

$$\Delta E_{v,3}=-0.16 .$$

Notice that $\Delta E_{v,1}+\Delta E_{v,2}+\Delta E_{v,3}=0$ (within the roundoff error), as appropriate for shifts expressed with respect to the average. We see that the uppermost valence band (v_1) in ZnS is 0.26 eV above $E_{v,\mathrm{av}}^{\mathrm{ZnS}}$. In ZnSe, the uppermost valence band is $\Delta_0/3=0.14$ eV above $E_{v,\mathrm{av}}^{\mathrm{ZnSe}}$. We previously had: $E_{v,\mathrm{av}}=0.70$ eV (higher in ZnSe). The final valence-band offset becomes: $\Delta E_v=0.70+0.14-0.26=0.58$ eV. The lineups are shown in Fig. 2.

B. Conduction bands

The procedure outlined above for valence bands also applies to degenerate conduction bands (with the simplification that no spin-orbit splitting enters). Direct conduction bands (at Γ) are nondegenerate and therefore only subject to hydrostatic strain shifts, as outlined in Sec. III. In semiconductors where the band gap is indirect, however, we need to analyze the strain splitting of the indirect conduction-band minima. These usually occur close to the X point (along the $\langle 001\rangle$ direction, also referred to as Δ) in the band structure (Si,AlAs,. . .), or at the L point ($\langle 111\rangle$ direction) (Ge). Because there are six equivalent $\langle 001\rangle$ directions, and eight $\langle 111\rangle$ directions, the conduction-band valleys all coincide in equilibrium, but can be split by the application of strain in appropriate directions. In that case, the value E_c^{ind} listed in Table II should be considered an average over the conduction-band valleys in spatially distinct directions. This average is shifted due to hydrostatic strains, using the a_c values listed in the table. Following the notation of Herring and Vogt,[39] the energy shift of valley i for a homogeneous deformation described by the strain tensor $\overleftrightarrow{\epsilon}$ can be expressed as

$$\Delta E_c^i=(\Xi_d\overleftrightarrow{1}+\Xi_u\{\hat{\mathbf{a}}_i\hat{\mathbf{a}}_i\}):\overleftrightarrow{\epsilon} , \tag{16}$$

where $\overleftrightarrow{1}$ is the unit tensor, $\hat{\mathbf{a}}_i$ is a unit vector parallel to the $\mathbf{k}$ vector of valley i, and $\{\ \}$ denotes a dyadic product. The shift of the mean energy of the conduction-band extrema is

$$\Delta E_{c,\mathrm{av}}=(\Xi_d+\tfrac{1}{3}\Xi_u)\overleftrightarrow{1}:\overleftrightarrow{\epsilon} . \tag{17}$$

The quantity $(\Xi_d+\frac{1}{3}\Xi_u)$, sometimes also denoted as E_1 (see Ref. 40), corresponds to a_c, the hydrostatic deformation potential for the conduction band (listed in Table II). Values of Ξ_u for selected semiconductors are listed in Table IV.

Starting from Eq. (16) we can once again express the shifts of individual bands with respect to the average $E_{c,\mathrm{av}}$. Conduction-band minima along Δ are not affected by uniaxial strain along (111). Under unaxial strain along (001) or (110), the bands along [100] and [010] split off from the one along [001]. The splittings of the bands with respect to the average is then given by

$$\Delta E_c^{001}=\tfrac{2}{3}\Xi_u^{\Delta}(\epsilon_{zz}-\epsilon_{xx}) , \tag{18a}$$

$$\Delta E_c^{100,010}=-\tfrac{1}{3}\Xi_u^{\Delta}(\epsilon_{zz}-\epsilon_{xx}) . \tag{18b}$$

The superscript Δ on Ξ_u indicates which type of conduction-band valley (at Δ or at L) we are considering, while the superscript on ΔE_c refers to the direction of the particular conduction-band minimum. Ξ_u is often denoted as E_2 (see Ref. 40).

Next we consider conduction bands at L. (001) strain has no effect now. Strain along [111] leads to

$$\Delta E_c^{111}=2\Xi_u^L\epsilon_{xy} , \tag{19a}$$

$$\Delta E_c^{\bar{1}11,1\bar{1}1,11\bar{1}}=-\tfrac{2}{3}\Xi_u^L\epsilon_{xy} . \tag{19b}$$

Finally, strain along [110] yields

$$\Delta E_c^{111,11\bar{1}}=+\tfrac{2}{3}\Xi_u^L\epsilon_{xy} , \tag{20a}$$

$$\Delta E_c^{\bar{1}11,1\bar{1}1}=-\tfrac{2}{3}\Xi_u^L\epsilon_{xy} . \tag{20b}$$

Values for Ξ_u are listed in Table IV. Ξ_u^L, like d, turns out to be sensitive to the value of the internal displacement parameter ζ.[11,29] Once again, the choice defined earlier appears to give good results. Note that experimental information is often only available for the lowest conduction-band minimum. Strain may cause a crossover in the band structure, however, requiring information on higher-lying bands. Calculated values are very useful in such cases.

V. DISCUSSION

A. Band offsets

In this section we will examine a number of technologically important examples of lattice-matched as well as strained-layer interfaces. Cases where reliable experimental values are available provide a good test of the

TABLE IV. Theoretical and experimental (Ref. 25) values for the deformation potentials Ξ_u^{Δ} and Ξ_u^L, for selected semiconductors. All values are in eV.

	Ξ_u^{Δ} (theor)	Ξ_u^{Δ} (expt)	Ξ_u^L (theor)	Ξ_u^L (expt)
Si	9.16	8.7	16.14	
Ge	9.42		15.13	16.3
GaAs	8.61		14.26	19.6
InAs	4.50		11.35	−3.6

model. I will also attempt to show how the model theory is useful for examining trends and quickly analyzing a wide variety of systems for specific applications.

As emphasized before, the model-solid theory was developed based on the results and insights provided by full self-consistent interface calculations for a wide variety of systems. Many lineups derived from Table II have been compared with results obtained from full self-consistent interface calculations, where available.[2,3,8,9,41,42] The results of the model are typically within 0.2 eV of the fully self-consistent values, both for lattice-matched and strained-layer interfaces. This theoretical justification, along with favorable comparisons with experiment, gives us confidence in the model and values presented here.

In Sec. III we used the example of AlSb/GaSb to illustrate the derivation of offsets at lattice-matched interfaces, and found $\Delta E_v = 0.47$ eV. This value is very close to the experimental value, 0.41 ± 0.1 eV, obtained by Gualtieri *et al.* from x-ray photoemission spectroscopy (XPS) measurements,[43] and 0.45 ± 0.08 eV, obtained by Menéndez *et al.* with a light-scattering technique.[44]

Our other example was that of a ZnS/ZnSe (001) interface, which resulted in a very small conduction-band offset: $\Delta E_c = 0.03$ eV. Because the model-solid theory is expressed in terms of analytical formulas and tabulated parameters, it lends itself easily to systematic studies of band offsets for a variety of situations. For instance, in the case of ZnS/ZnSe one might want to explore whether variations in the strain (created by growth on different substrates, or in free-standing superlattices with various layer thicknesses) can lead to significant variations in the conduction-band offset, perhaps with the goal of developing a device structure for which a sizable ΔE_c is essential. In the case of ZnS/ZnSe, we find that the conduction-band offset is always small. This prediction was confirmed by experimental observations.[45] Model-solid predictions for other II-VI compound interfaces are discussed in Ref. 41.

The list of cases where model-solid predictions agree well with experiment is long and still growing. Very good results were found for Si/Ge strained-layer interfaces, as discussed in Ref. 9. Many lattice-matched junctions were discussed in Ref. 2. As an example, ΔE_v for AlAs/GaAs is predicted to be 0.60 eV, and measured as 0.45–0.56 eV.[46–48] For InAs/GaSb, the model predicts the correct "broken gap" lineup, with the valence band of GaSb above the conduction band of InAs. In the case of CdTe/HgTe, the model solid[42] favors the "large valence-band offset," giving $\Delta E_v = 0.24$ eV (to be compared with the x-ray photoemission value[49] of $\Delta E_v = 0.35$ eV).

Heterostructures are often based not only on pure materials, but also on alloys. Varying the composition of an alloy yields variations in the lattice constant, which are well described by a linear interpolation such as in the virtual-crystal approximation. This provides additional flexibility in tailoring the electronic properties of the system. To derive valence-band positions for an alloy, linear interpolation between the pure materials is appropriate. This approach comes naturally in the context of superposition of atoms in the model solid. When the constituent materials are not lattice matched, one should actually also consider a strain contribution, since in an alloy $A_xB_{1-x}C$ [with lattice constant $a_0 = xa_0(AC) + (1-x)a_0(BC)$] one material is effectively expanded, whereas the other is compressed. For an energy level E_i, with deformation potentials a_i, this leads to the following expression:[50]

$$E(x) = xE(AC) + (1-x)E(BC) + 3x(1-x)[-a_i(AC) + a_i(BC)]\frac{\Delta a}{a_0} , \quad (21)$$

where $\Delta a = a_0(AC) - a_0(BC)$.

The linear-interpolation approximation may be less adequate for conduction bands. In cases where large bowing is present (i.e., nonlinear behavior of the band gap as a function of alloy composition) I recommend the use of experimental values for the alloy band gap (including bowing), in conjunction with model-solid values for valence-band positions. Strain-induced shifts of the bands in the alloy can always be reliably predicted using linearly-interpolated values of deformation potentials.

Heterostructures based on combinations of GaAs, InAs, and InP are attracting increasing attention. As an example, we consider lattice-matched $Ga_{0.47}In_{0.53}As$ grown on a (100) InP substrate and find [with Eq. (21)] $\Delta E_v = 0.35$ eV. Lang *et al.*[51] applied the novel technique of admittance spectroscopy to this lattice-matched interface, leading to a valence-band offset of 0.35 eV. Skolnick *et al.*[52] found $\Delta E_v = 0.38$ eV in an optical spectroscopy study. Forrest *et al.*,[53] using capacitance-voltage (C-V) techniques, obtained $\Delta E_v = 0.36$ eV. They also established that the relationship $\Delta E_c = 0.40\Delta E_g$ holds for a series of lattice-matched InGaAsP/InP interfaces, spanning the alloy range from $In_{0.53}Ga_{0.47}As$ to pure InP. Finally, Westland *et al.*[54] reported optical absorption and photoluminescence measurements on $Ga_{0.47}In_{0.43}As$/InP quantum wells, leading to $\Delta E_v = 0.325$ eV. All these values are in excellent agreement with the theoretical prediction.

Only one publication seems to give a somewhat different result, namely the photoluminescence experiments of Sauer *et al.* on $In_{0.53}Ga_{0.47}As$/InP quantum wells.[55] They report $\Delta E_v = 0.40\Delta E_g$ (and $\Delta E_c = 0.60\Delta E_g$), and consider this inconsistent with other experimental offsets (quoted above). However, with the ΔE_g value used in their work we find $\Delta E_v = 0.25$ eV. This is only 0.1 eV different from other values (and the model theory), which seems to be within the error bar of even the most reliable experiments to date.

When the composition of the $Ga_xIn_{1-x}As$ alloy is changed, strains are introduced during pseudomorphic growth on a InP substrate. The band alignments in the resulting heterostructures have recently been analyzed by People,[56] using our values for the lineups. Gershoni *et al.* have performed low-temperature photoluminescence and photocurrent experiments on such $In_xGa_{1-x}As$/InP strained-layer superlattices.[57] Good agreement with their data is obtained if they assume a valence-band offset for the lattice-matched system of 59% of the band-gap discontinuity; a 15% variation in

this value does not cause any appreciable change in the calculated curves, however. With the ΔE_g value used in their paper, $\Delta E_v = 0.59 \Delta E_g$ leads to $\Delta E_v = 0.37$ eV for $Ga_{0.47}In_{0.53}As/InP$, in very good agreement with the other experiments, and with the theoretical value.

A word of caution is appropriate here: when experimental data for band offsets are expressed as a percentage of the band-gap discontinuity ΔE_g, it is important to check which values for the band gaps were used by the authors. These values may be different from the ones listed in Table II, due to several reasons: different measurement temperature (values in Table II are for low temperatures), or bowing which causes a derivation from linearity. To compare with the theory, one should use the ΔE_g value quoted in the experimental work to calculate ΔE_v (in eV).

A closely related system is that of $Al_{0.48}In_{0.52}As/Ga_{0.47}In_{0.53}As$, which was examined by People *et al.*[58] using a *C-V* profiling technique. They found $\Delta E_c = 0.50$ eV, and $\Delta E_v = 0.20$ eV. Using Eq. (21), we obtain with the model-solid values, $\Delta E_v = 0.21$ eV, in good agreement with the experimental value. Rao *et al.*[59] used *C-V* profiling to measure valence- and conduction-band discontinuities at the lattice-matched $Ga_{0.51}In_{0.49}P/GaAs$ interface. They found $\Delta E_v = 0.24$ eV. Our theoretical value is 0.36 eV.

Smith and Mailhiot have recently proposed $InAs/Ga_{0.6}In_{0.4}Sb$ superlattices as novel infrared photodetectors.[60] In their analysis, they assume that the valence bands of unstrained InSb and GaSb line up. From Table II we see that the theory predicts the valence band of InSb to be higher in energy by 0.16 eV than the valence band of GaSb (the spin-orbit splitting is similar in both). This actually implies that the predicted properties of the superlattices are better than for the band offset used by Smith and Mailhiot. Based on Table II, we predict a value for $E_{v,av}$ at a $InAs/Ga_{0.6}In_{0.4}Sb$ heterojunction of ~ 0.48 eV. Note that this can lead to a "broken-gap" lineup of the type that occurs in InAs/GaSb, but also that strain-induced shifts and splittings of the bands can lead to widely different values for ΔE_v.

B. Band-edge deformation potentials

The values for band-edge deformation potentials listed in Table II have already been used extensively in our predictions of band offsets at strained-layer interfaces. The good agreement with experiment obtained in many test cases already provides an indication of the reliability of these values. I also pointed out that the model-solid deformation potentials agree very well with values obtained from fully self-consistent calculations that produce the actual displacement of the band edges due to an inhomogeneous deformation of the crystal.[7] It is interesting, however, to investigate the practical significance of these values in their own right.

While values for the band-gap deformation potentials can be directly compared with reliable experimental data, the individual band-edge deformation potentials a_v and a_c are much harder to obtain experimentally, and have been quite controversial. Measurements are indirect, and require a significant amount of analysis and interpretation, including some assumptions. Here I will only mention some of the recent results; a more detailed discussion is presented in Ref. 7.

In principle, the deformation potentials can be determined from mobility measurements on high-purity materials. Only in GaAs does there seem to be a growing consensus about the value for $|a_c|$ determined in this fashion, which is around 7 eV.[61] The model-solid value is $a_c = -7.17$ eV.

A second class of measurements is based on the use of transition-metal impurity levels as reference levels in band-structure lineups. This approach relies on the observation that several substitutional transition metal impurities give rise to deep levels that exhibit a universal behavior, i.e., they can serve as reference lineups to line up band structures at heterojunctions.[62] At this point in time, no rigorous theoretical justification exists for this approach, and no information is available about its generality and accuracy. Based on its success for a number of heterojunctions, however, it seems attractive to apply the approach to the deformation potential problem. Based on their own DLTS experiments, Nolte *et al.*[63] found a value of $a_c = -9.3$ eV for GaAs, and -7.0 eV for InP. They also derived a value of $a_c = 2.4$ eV for Si, based on other published work.[64] In a similar approach, Samuelson and Nilsson[65] used photoluminescence to determine the hydrostatic pressure derivatives, and found $a_c = -7.7$ eV in GaAs. All of these values are in reasonable agreement with the present first-principles calculations.

A third class of measurements relies on the effect of heavy doping on the lattice constant. A large concentration of shallow donors, for instance, can lead to a volume change which lowers the conduction band, and reduces the total energy of the system. This effect has to compete, of course, with the increase in elastic energy; formulas have been developed by Yokota.[66] The change in lattice constant in general not only depends on this electronic effect, but also includes a "size effect" due to the presence of a different type of atoms. A way of separating these effects was proposed in recent work by Cargill *et al.*, who used x-ray scattering to determine the changes in lattice constant, and extended x-ray absorption fine-structure (EXAFS) measurements to extract the size effect.[67] For Si, they found $a_c = 3.3$ eV, very close to the theoretical value.

With regard to other theories, we can compare the values of band-edge deformation potentials listed in Table II with those obtained by Cardona and Christensen[68] based on a dielectric screening model. There appears to be a remarkable difference between the values for the valence-band deformation potentials: ours are all positive, whereas those obtained by Cardona and Christensen are all negative. All these values are quite small in magnitude, however, so that the difference may not be very significant. The model-solid values show better agreement with the most recent experiments.

An important overall conclusion to be drawn from Table II is that the valence-band deformation potentials are small compared to the deformation potentials for the

direct gap; for direct-gap semiconductors, most of the variation under strain occurs in the conduction band.

C. Pressure dependence of band offsets

The values in Table II allow the derivation of band discontinuities, including cases where strains are present. So far, we have only considered situations where these strains are built in, due to a lattice mismatch. The approach can also be used, however, in the case of externally applied pressure. The investigation of heterojunctions under pressure is indeed becoming an important experimental tool.[69–71]

Theoretical values for changes in band offsets at lattice-matched interfaces under applied hydrostatic pressure can be obtained by taking differences of the band-edge deformation potentials listed in Table II. When this procedure is applied to valence-band offsets, the resulting pressure derivative will be small because the individual numbers for the valence bands are similar in magnitude. Since they are also subject to an error bar of ± 1 eV, the relative error will be rather large. For AlAs/GaAs we obtain from Table II: $[d(\Delta E_v)]/[d\ln\Omega] = a_v^{\mathrm{GaAs}} - a_v^{\mathrm{AlAs}} = -1.31$ eV. Self-consistent interface calculations for this system under hydrostatic pressure[2] produced a value $[d(\Delta E_v)]/[d\ln\Omega] = -0.64$ eV. We see that the difference between model-solid theory and full calculations is well within the error bar. The result that $[d(\Delta E_v)]/[d\ln\Omega]$ is small indicates that ΔE_v remains rather constant under pressure, an assumption essential for the interpretation of the experiments in Ref. 69.

Another very interesting case is that of InAs/GaSb, which has a so-called staggered lineup: the GaSb valence band is higher in energy than the InAs conduction band. Investigators therefore often concentrate upon the measurement of the energy difference between these two bands. Claessen *et al.*[70] used magneto-optical methods to determine the change in energy separation between E_c^{InAs} and E_v^{GaSb} under hydrostatic pressure, and found $d(E_v^{\mathrm{GaSb}} - E_c^{\mathrm{InAs}})/dP = -5.8$ meV/kbar. From an analysis of transport measurements on InAs/GaSb heterostructures under hydrostatic pressure, Beerens *et al.*[71] derived

$$d(E_v^{\mathrm{GaSb}} - E_c^{\mathrm{InAs}})/dP = -67 \text{ meV/GPa} = -6.7 \text{ meV/kbar} .$$

Using the values from Table II, we find that

$$d(E_v^{\mathrm{GaSb}} - E_c^{\mathrm{InAs}})/d\ln\Omega = (0.79) - (-5.08) = 5.87 \text{ eV} .$$

This value was confirmed by carrying out a full self-consistent interface calculation, which agreed with the model solid to within 0.3 eV. The theoretical values are expressed as energy shifts per fractional volume change. In order to convert to energy shifts per unit pressure, one can use the relationship $P = -B\Delta\Omega/\Omega$, where B is the bulk modulus. B can quite easily be obtained from Table I, using the formula $B = (c_{11} + 2c_{12})/3$. This leads to $B = 580$ kbar for InAs, and $B = 578$ kbar for GaSb. We thus find $d(E_v^{\mathrm{GaSb}} - E_c^{\mathrm{InAs}})/dP = -10.1$ meV/kbar. The error bar on the a_v and a_c values in Table II is ± 1 eV, which leads to an error bar of ± 3 meV on the value of the pressure derivative. Because of the error bar on the theoretical (and presumably also on the experimental) value, the theoretical result is not inconsistent with the experiments quoted above. However, the deviation may indicate that other factors are playing a role in the experiment or its interpretation. One possible factor is uniaxial strain. The theoretical value is derived under the assumption that the strain is purely hydrostatic. In the experimental situation, even if the applied stress is purely hydrostatic, small uniaxial components may arise because of the anisotropy of the sample (e.g., due to the difference in elastic constants between the two materials). Uniaxial strain does not affect the InAs conduction band, but leads to a splitting of the GaSb valence bands; this may reduce the observed rate of decrease of the band discontinuity.

VI. CONCLUSIONS

I have presented a theoretical model to calculate band lineups at lattice-matched and strained-layer interfaces, and tabulated parameters to calculate band lineups for a wide variety of semiconductors. The important effects due to strains in the layers were emphasized, and prescriptions for evaluating the strain components were given. These strains are determined by the lattice constants (i.e., choice of materials and alloy composition), the boundary conditions (i.e., choice of substrate), and the thickness of the layers (in a free-standing superlattice). This provides wide flexibility in the design of new heterostructures. The model-solid theory, developed based on full self-consistent interface calculations, compares well with experiment in various reliable test cases. The model and values presented here therefore provide a basis for analysis and design of novel interface structures, as illustrated in many examples.

ACKNOWLEDGMENTS

Thanks are due to R. M. Martin for continued support, to D. J. Chadi for providing me with results of tight-binding calculations, and to J. Tersoff and W. A. Harrison for helpful discussions and suggestions.

*Present address: Philips Laboratories, North American Philips Corporation, 345 Scarborough Road, Briarcliff Manor, NY 10510.

[1] G. C. Osbourn, J. Appl. Phys. **53**, 1586 (1982).

[2] C. G. Van de Walle and R. M. Martin, Phys. Rev. B **35**, 8154 (1987).

[3] C. G. Van de Walle and R. M. Martin, Phys. Rev. B **34**, 5621 (1986).

[4]See the discussion in Ref. 2.
[5]J. Bardeen and W. Shockley, Phys. Rev. **80**, 72 (1950).
[6]R. M. Martin and C. G. Van de Walle, Bull. Am. Phys. Soc. **30**, (3), 226 (1987).
[7]C. G. Van de Walle and R. M. Martin (unpublished).
[8]C. G. Van de Walle, Ph.D. dissertation, Stanford University, 1986.
[9]C. G. Van de Walle and R. M. Martin, J. Vac. Sci. Technol. B **4**, 1055 (1986).
[10]L. C. Feldman, J. Bevk, B. A. Davidson, H.-J. Gossman, and J. P. Mannaerts, Phys. Rev. Lett. **59**, 664 (1987).
[11]L. Kleinman, Phys. Rev. **128**, 2614 (1962).
[12]H. J. McSkimin, J. Appl. Phys. **24**, 988 (1953); H. J. McSkimin and P. Andreatch, Jr., *ibid.* **35**, 3312 (1964).
[13]C. W. Garland and K. C. Park, J. Appl. Phys. **33**, 759 (1962).
[14]J. D. Wiley, in *Semiconductors and Semimetals,* edited by R. K. Willardson and A. C. Beer (Academic, New York, 1975), Vol. 10.
[15]D. Gerlich, J. Appl. Phys. **34**, 813 (1963).
[16]W. F. Boyle and R. J. Sladek, Phys. Rev. B **11**, 2933 (1975).
[17]F. S. Hickernell and W. R. Gayton, J. Appl. Phys. **37**, 462 (1966).
[18]W. F. Boyle and R. J. Sladek, Phys. Rev. B **11**, 1587 (1975).
[19]D. I. Bolef and M. Menes, J. Appl. Phys. **31**, 1426 (1960).
[20]I. O. Bashkin and G. I. Pereseda, Fiz. Tverd. Tela (Leningrad) **16**, 3166 (1974) [Sov. Phys.—Solid State **16**, 2058 (1975)].
[21]D. Berlincourt, H. Jaffe, and L. R. Shiozawa, Phys. Rev. **129**, 1009 (1963).
[22]R. B. Hall and J. D. Meakin, Thin Solid Films **63**, 203 (1979).
[23]R. D. Greenough and S. B. Palmer, J. Phys. D **6**, 587 (1973).
[24]R. I. Cottam and G. I. Saunders, J. Phys. Chem. Solids **36**, 187 (1975).
[25]*Landolt-Börnstein, Numerical Data and Functional Relationships in Science and Techology* (Springer, New York, 1982), Group III, Vol. 17a-b.
[26]W. A. Harrison, E.A. Kraut, J. R. Waldrop, and R. W. Grant, Phys. Rev. B **18**, 4402 (1978); R. M. Martin, J. Vac. Sci. Technol. **17**, 978 (1980).
[27]K. Kunc and R. M. Martin, Phys. Rev. B **24**, 3445 (1981).
[28]P. Hohenberg and W. Kohn, Phys. Rev. **136**, B864 (1964); W. Kohn and L. J. Sham, *ibid.* **140**, A1133 (1965); exchange and correlation potentials are based on the data from D. M. Ceperley and B. J. Alder, Phys. Rev. Lett. **45**, 566 (1980), as parametrized by J. Perdew and A. Zunger, Phys. Rev. B **23**, 5048 (1981).
[29]See, e.g., O. H. Nielsen and R. M. Martin, Phys. Rev. B **32**, 3792 (1985).
[30]G. B. Bachelet, D. R. Hamann, and M. Schlüter, Phys. Rev. B **26**, 4199 (1982).
[31]Although the absolute position of conduction bands suffers from large errors, *changes* in the bands such as those induced by uniaxial or hydrostatic pressure are still reliably predicted. This feature will be used in calculating conduction-band deformation potentials.
[32]Recent quasiparticle-energy calculations confirm this assessment; see M. S. Hybertsen and S. G. Louie, Phys. Rev. B **34**, 5390 (1986).
[33]L. Kleinman, Phys. Rev. B **24**, 7412 (1981).
[34]The electrostatic potential is, of course, only one part of the total potential in the solid; one also has to include the exchange and correlation potential. Since the latter is not linear in the charge density, it cannot be obtained from a superposition of atoms. However, this term is well defined in a bulk calculation for the solid, since it is short range in nature (it is the long-range terms which cause the arbitrariness in the electrostatic potential). It can therefore be taken directly from the bulk calculation, and only the electrostatic part of the potential should be obtained from the "model solid." When strain is present, the exchange and correlation potential can be obtained from the value for the unstrained material, using the property that it is roughly proportional to $\rho^{1/3}$. It can therefore to a good approximation be considered to vary as $\Omega^{-1/3}$.
[35]Atomic configurations are listed in Ref. 2, and were obtained from tight-binding calculations by D. J. Chadi (private communication). The sensitivity of the model-solid values to the choice of configuration was discussed in Ref. 2.
[36]C. G. Van de Walle and R. M. Martin, Phys. Rev. B **37**, 4801 (1988).
[37]F. H. Pollak and M. Cardona, Phys. Rev. **172**, 816 (1968).
[38]D. W. Langer, R. N. Euwema, K. Era, and T. Koda, Phys. Rev. B **2**, 4005 (1970).
[39]W. C. Herring and E. Vogt, Phys. Rev. **101**, 944 (1956); I. Balslev, *ibid.* **143**, 636 (1966).
[40]E. O. Kane, Phys. Rev. **178**, 1368 (1969).
[41]C. G. Van de Walle, K. Shahzad, and D. J. Olego, J. Vac. Sci. Technol. B **6**, 1350 (1988).
[42]C. G. Van de Walle and R. M. Martin, J. Vac. Sci. Technol. B **5**, 1225 (1987).
[43]G. P. Gualtieri, R. G. Nuzzo, R. J. Malik, J. F. Walker, L. C. Feldman, W. A. Sunder, and G. P. Schwartz, J. Vac. Technol. B **5**, 1284 (1987).
[44]J. Menéndez, A. Pinczuk, D. J. Werder, J. P. Valladares, T. H. Chiu, and W. T. Tsang, Solid State Commun. **61**, 703 (1987).
[45]K. Shahzad, D. J. Olego, and C. G. Van de Walle, Phys. Rev. B **38**, 1417 (1988).
[46]W. I. Wang and F. Stern, J. Vac. Sci. Technol. B **3**, 1280 (1985).
[47]J. Batey and S. L. Wright, J. Appl. Phys. **59**, 200 (1986).
[48]D. J. Wolford, in *Proceedings of the 18th International Conference on the Physics of Semiconductors,* edited by O. Engström (World Scientific, Singapore, 1987), p. 1115.
[49]S. P. Kowalczyk, J. T. Cheung, E. A. Kraut, and R. W. Grant, Phys. Rev. Lett. **56**, 1605 (1986).
[50]M. Cardona and N. E. Christensen, Phys. Rev. B **37**, 1011 (1988).
[51]D. V. Lang, M. B. Panish, F. Capasso, J. Allam, R. A. Hamm, A. M. Sergent, and W. T. Tsang, Appl. Phys. Lett. **50**, 736 (1987).
[52]M. S. Skolnick, P. R. Tapster, S. J. Bass, A. D. Pitt, A. Apsley, and S. P. Aldred, Semicond. Sci. Technol. **1**, 29 (1986).
[53]S. R. Forrest, P. H. Schmidt, R. B. Wilson, and M. L. Kaplan, Appl. Phys. Lett. **45**, 1199 (1984).
[54]D. J. Westland, A. M. Fox, A. C. Maciel, J. R. Ryan, M. D. Scott, J. I. Davies, and J. R. Riffat, Appl. Phys. Lett. **50**, 839 (1987).
[55]R. Sauer, T. D. Harris, and W. T. Tsang, Phys. Rev. B **34**, 9023 (1986).
[56]R. People, J. Appl. Phys. **62**, 2551 (1987).
[57]D. Gershoni, J. M. Vandenberg, R. A. Hamm, H. Temkin, and M. B. Panish, Phys. Rev. B **36**, 1320 (1987).
[58]R. People, K. W. Wecht, K. Alavi, and A. Y. Cho, Appl. Phys. Lett. **43**, 118 (1983).
[59]M. A. Rao, E. J. Caine, H. Kroemer, S. I. Long, and D. I. Babic, J. Appl. Phys. **61**, 643 (1987).
[60]D. L. Smith and C. Mailhiot, J. Appl. Phys. **62**, 2545 (1987).
[61]W. Walukiewicz, H. E. Ruda, J. Lagowski, and H. C. Gatos,

Phys. Rev. B **32**, 2645 (1985).
[62]M. J. Caldas, A. Fazzio, and A. Zunger, Appl. Phys. Lett. **45**, 671 (1984); J. M. Langer and H. Heinrich, Phys. Rev. Lett. **55**, 1414 (1985).
[63]D. D. Nolte, W. Walukiewicz, and E. E. Haller, Phys. Rev. Lett. **59**, 501 (1987).
[64]D. D. Nolte, W. Walukiewicz, and E. E. Haller, Phys. Rev. B **36**, 9392 (1987).
[65]L. Samuelson and S. Nilsson, J. Lumin. **40&41**, 127 (1988).
[66]I. Yokota, J. Phys. Soc. Jpn. **18**, 1487 (1964).
[67]G. S. Cargill III, J. Angilello, and K. L. Kavanagh, Phys. Rev. Lett. **61**, 1748 (1988).
[68]M. Cardona and N. E. Christensen, Phys. Rev. B **35**, 6182 (1987); **36**, 2906(E) (1987).
[69]D. J. Wolford, T. F. Kuech, J. A. Bradley, M. Jaros, M. A. Gell, and D. Ninno, J. Vac. Sci. Technol. B **4**, 1043 (1986); U. Venkateswaran, M. Chandrasekhar, H. R. Chandrasekhar, B. A. Vojak, F. A. Chambers, and J. M. Meese, Phys. Rev. B **33**, 8416 (1986).
[70]L. M. Claessen, J. C. Maan, M. Altarelli, P. Wyder, L. L. Chang, and L. Esaki, Phys. Rev. Lett. **57**, 2556 (1986).
[71]J. Beerens, G. Grégoris, J. C. Portal, E. E. Mendez, L. L. Chang, and L. Esaki, Phys. Rev. B **36**, 4742 (1988).